The EMBO Journal (2011) 30, 2044–2056 | © 2011 European Molecular Biology Organization | All Rights Reserved 0261-4189/11
www.embojournal.org

THE EMBO JOURNAL

Glutathione revisited: a vital function in iron metabolism and ancillary role in thiol-redox control

Chitranshu Kumar[1,5], Aeid Igbaria[1,5], Benoît D'autreaux[1,2], Anne-Gaëlle Planson[1], Christophe Junot[3], Emmanuel Godat[3], Anand K Bachhawat[4], Agnès Delaunay-Moisan[1] and Michel B Toledano[1,*]

[1]LSOC, DSV, IBITECS, CEA-Saclay, France, [2]ICSN, CNRS UPR2301, Gif-sur-Yvette, France, [3]LEMM, DSV, IBITECS, CEA-Saclay, France and [4]Institute of Microbial Technology, Chandigarh, India

Glutathione contributes to thiol-redox control and to extra-mitochondrial iron–sulphur cluster (ISC) maturation. To determine the physiological importance of these functions and sort out those that account for the GSH requirement for viability, we performed a comprehensive analysis of yeast cells depleted of or containing toxic levels of GSH. Both conditions triggered an intense iron starvation-like response and impaired the activity of extra-mitochondrial ISC enzymes but did not impact thiol-redox maintenance, except for high glutathione levels that altered oxidative protein folding in the endoplasmic reticulum. While iron partially rescued the ISC maturation and growth defects of GSH-depleted cells, genetic experiments indicated that unlike thioredoxin, glutathione could not support by itself the thiol-redox duties of the cell. We propose that glutathione is essential by its requirement in ISC assembly, but only serves as a thioredoxin backup in cytosolic thiol-redox maintenance. Glutathione-high physiological levels are thus meant to insulate its cytosolic function in iron metabolism from variations of its concentration during redox stresses, a model challenging the traditional view of it as prime actor in thiol-redox control.

The EMBO Journal (2011) **30,** 2044–2056. doi:10.1038/emboj.2011.105; Published online 8 April 2011
Subject Categories: cellular metabolism
Keywords: glutathione; iron–sulphur cluster; oxidative protein folding; redox homoeostasis; thioredoxin

Introduction

The low-molecular weight thiol glutathione (L-γ-glutamyl-L-cysteinylglycine) (GSH), glutathione reductase and glutaredoxin constitute with the thioredoxin pathway, the two independent arms of the system that assists disulphide bond reduction (Toledano *et al*, 2007). Because of its high cellular abundance, between 3 and 10 mM, and low redox potential of −240 mV, GSH is also given the special attribute of a redox buffer not only important for reducing oxidized cysteine residues, but also for protecting them from irreversible oxidation and for scavenging various endogenous and exogenous electrophilic compounds (Meister and Anderson, 1983; Grant *et al*, 1999; Shelton and Mieyal, 2008).

In *E. coli*, simultaneous inactivation of the GSH and thioredoxin pathways is unviable but inactivation of either pathway is fully viable, which indicate that each can fully operate the essential function of reducing disulphides in the absence of the other (reviewed in Toledano *et al* (2007)). In *S. cerevisiae*, inactivating glutathione reductase together with both cytoplasmic thioredoxins (Muller, 1996) or with thioredoxin reductase (Trotter and Grant, 2003) is also lethal, whereas deletion of both cytoplasmic thioredoxins (Muller, 1991) or of both dithiol glutaredoxins (Luikenhuis *et al*, 1998) is viable. However, unlike in *E. coli*, deletion of the rate-limiting GSH-biosynthetic enzyme, γ-glutamyl cysteine synthase (*gsh1*Δ) is unviable on its own (Wu and Moye-Rowley, 1994; Grant *et al*, 1996). Such a requirement of GSH for yeast viability has prevented evaluating its contribution to thiol-redox control, and constitutes an enigma as to its molecular cause. Attempts at identifying yeast extragenic suppressors of the GSH auxotrophy of *gsh1*Δ only yielded mutations restoring synthesis of very small GSH amounts, indicating both that no single-gene mutation can replace GSH and that minute amounts of the tripeptide suffice for full viability (Spector *et al*, 2001). A reactive oxygen species (ROS)-protective function cannot account for the yeast GSH requirement, as anaerobiosis does not rescue GSH auxotrophy (Spector *et al*, 2001). Ribonucleotide reduction is the function that makes the presence of either the GSH or thioredoxin pathways essential for *E. coli* aerobic viability (Gon *et al*, 2006b), but is predominantly operated by thioredoxin in yeast (Camier *et al*, 2007). In the endoplasmic reticulum (ER), GSH competes with luminal protein-thiols for oxidation by the ER oxidase (Ero1)-protein disulphide isomerase (Pdi1) oxidative folding machinery (Cuozzo and Kaiser, 1999), but ER secretion is not altered by GSH depletion (Frand and Kaiser, 1998; Pollard *et al*, 1998). If not for thiol-redox maintenance, GSH might otherwise be essential by its requirement, together with the mitochondrial inner-membrane ABC transporter Atm1 and the intermembrane space Erv1 thiol oxidase, for maturation of cytoplasmic iron–sulphur cluster (ISC) by the cytosolic ISC assembly (CIA) system (Kispal *et al*, 1999; Lange *et al*, 2001; Sipos *et al*, 2002), which is a vital process (Lill, 2009).

In addition to its essential nature, GSH impedes growth when at high intracellular levels, as suggests the inability of yeast cells overexpressing Hgt1, a specific GSH transporter (Bourbouloux *et al*, 2000), to grow on medium containing GSH (Srikanth *et al*, 2005).

*Corresponding author. LSOC, IBITECS, CEA-Saclay, Bat142, 91191 Gif-sur-Yvette, Essonne, France. Tel.: +33 16 908 8244; Fax: +33 16 908 8046; E-mail: michel.toledano@cea.fr
[5]These authors contributed equally to this work

Received: 27 September 2010; accepted: 17 March 2011; published online: 8 April 2011

To apprehend the physiological role of GSH, we sought to elucidate the bases of its essential requirement and toxicity by analysing the cellular consequences of its depletion and presence at toxic levels, using the *gsh1*Δ and *HGT1*-overexpressing strains, respectively. Both extreme GSH conditions caused major alterations of iron metabolism, but surprisingly did not significantly impact thiol-redox control, except for the effect of high GSH levels blocking oxidative protein folding and secretion. We also evaluated the contribution of GSH to thiol-redox maintenance by the redox load excess of cells with a crippled thioredoxin pathway and, conversely, tested the effect of exogenous iron in rescuing the defects of GSH-depleted cells. Altogether, our data indicate that the essential function of GSH is linked to its involvement in iron metabolism, which requires very limited amounts of the tripeptide, while its cytosolic thiol-redox function only serves as backup of thioredoxin, and requires high levels of the tripeptide. We further show that such split functions of GSH link thiol-redox control and iron metabolism thereby causing redox stresses that consume GSH to impinge on iron metabolism. We propose a model that departs from the notion of GSH as a prime actor in thiol-redox maintenance, while emphasizing its crucial role in iron metabolism.

Results

HGT1 overexpression causes toxic accumulation of GSH

Hgt1 is an exclusive GSH and GSSG transporter (Bourbouloux *et al*, 2000). Cells that overexpressed *HGT1* were unable to grow on minimal medium plates that contained GSH at concentrations as low as 20 μM (Figure 1A). Similarly in liquid medium, HGT1 cells were growth inhibited at GSH concentrations of 50 μM and above (Figure 1B), but then resumed growth after a few hours. These cells died massively within 4 h after GSH addition (Figure 1C). Lack of a dose effect on cell killing at GSH concentration above 100 μM probably reflects saturation of HGT1, the Km of which for GSH is 50 μM (Bourbouloux *et al*, 2000). Saturation of GSH uptake also explains the lag period before growth resumption to be longer at 200 μM than at 100 μM GSH, as GSH remains longer in the medium under the former condition. In the absence of GSH, HGT1 cells had a wild-type GSH content (7.5 mM); however, on adding GSH (100 μM), this concentration peaked at ∼70 mM after 30 min (Figure 1D; Table I). GSSG levels paralleled the increase in GSH levels peaking at 1.7 mM from a baseline value of 0.2 mM. The increases in GSH and GSSG resulted in a significant decrease of the GSH redox potential (E_{GSH}) from approximately −220 mV to approximately −250 mV at 30 min. GSH levels then decreased after an hour to normalize at 8 h (Figure 1D; Table I). Such decrease, which explains the growth resumption of HGT1 cells in liquid medium and only partial lethality (see Figure 1B and C), is not a consequence of GSH efflux, as the GSH concentration in the culture medium gradually decreased (Supplementary Figure S1A), but of degradation by the γ-glutamyl transpeptidase (γ-GT)-independent Dug1–Dug2–Dug3 pathway (Ganguli *et al*, 2007; Kaur *et al*, 2009), as the corresponding mutants maintained elevated GSH levels for a longer period and were sensitive to lower GSH concentrations (Supplementary Figure S1B and C). The decreased GSH tolerance

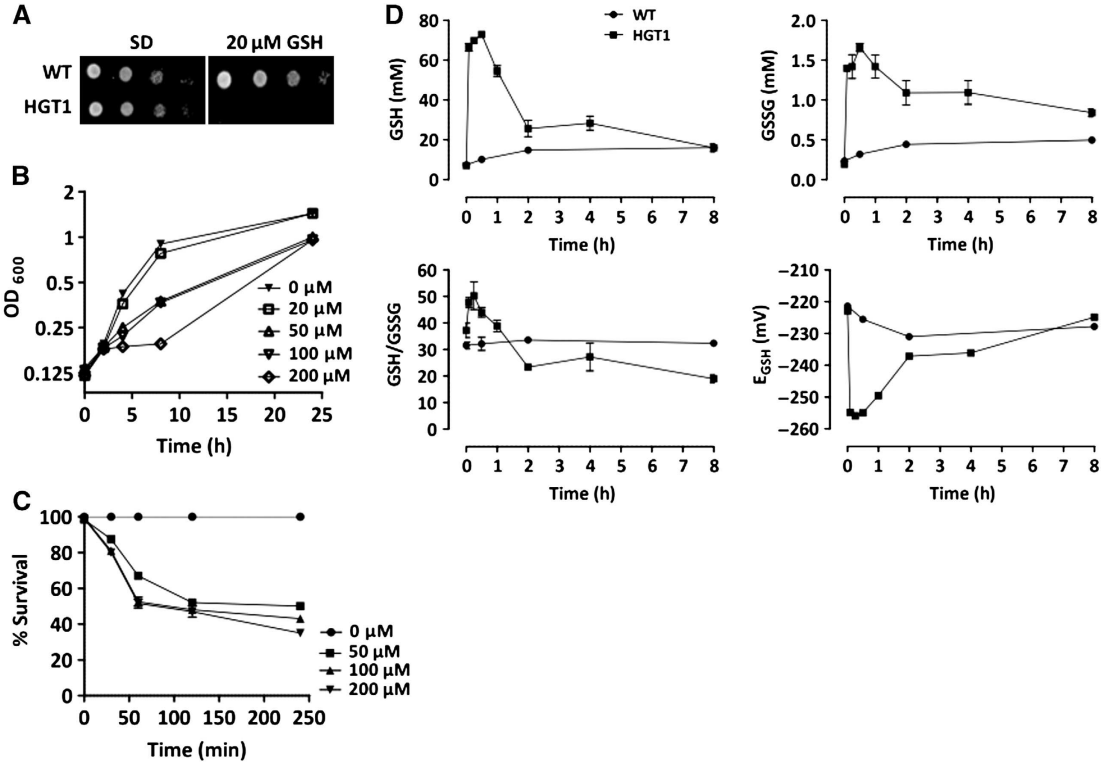

Figure 1 *HGT1* overexpression increases GSH to toxic levels. (**A**) HGT1 or WT cells serially diluted and spotted onto SD plates containing or not containing GSH (20 μM). (**B**) HGT1 cells inoculated in fresh SD medium containing GSH, as indicated and growth monitored by turbidity. (**C**) HGT1 cells incubated in SD medium containing the indicated amount of GSH for the indicated time, and spread onto SD plates lacking GSH. Colony forming units were recorded (% survival relative to untreated cells). (**D**) Kinetics of cellular content of GSH (upper left), GSSG (upper right), GSH/GSSG (lower left) and GSH redox potential (E_{GSH}) (lower right) in HGT1 and WT cells grown in SD medium supplemented with GSH (100 μM). GSH and GSSG in mM/cell. Values are the mean of three independent experiments. Error bars represent mean values ± s.d.

Table I GSH measurements in HGT1 and *gsh1*Δ cells

Strain	GSH added[a]	[GSH] (mM/cell)	[GSSG] (mM/cell)	GSH/GSSG	E_{GSH} (mV)
WT	0	7.2 ± 0.04	0.21 ± 0.02	31 ± 1.25	−221.78 ± 0.65
HGT1	0	7.59 ± 0.27	0.19 ± 0.02	38.94 ± 4.94	−224.02 ± 2.03
HGT1	50 μM	35.13 ± 3.49	0.9 ± 0.02	39.08 ± 4.49	−244.03 ± 2.88
HGT1	100 μM	54.53 ± 4.61	1.42 ± 0.06	38.86 ± 3.75	−249.56 ± 2.88
*gsh1*Δ	100 μM	2.17 ± 0.07	0.08	26.72 ± 0.37	−202.80 ± 0.51
*gsh1*Δ	1 μM	0.43 ± 0.05	0.03	16.49 ± 1.23	−175.27 ± 2.61
*gsh1*Δ	0	0.06 ± 0.002	0.02	2.92 ± 0.06	−125.44 ± 0.52
*trr1*Δ	0	11.46 ± 1.2	1.34 ± 0.04	8.57 ± 1.11	−209.69 ± 0.62

[a]In HGT1 cells, GSH and GSSG measurements were performed 1 h after GSH addition; in *gsh1*Δ: in exponentially grown cells in the presence of the indicated GSH amount or in cells grown for six divisions in SD medium lacking GSH; in *trr1*Δ: in exponentially growing cells. Data are from three replicate samples of independent cultures ± s.d.

of the Dug pathway mutants indicates that GSH toxicity is caused by GSH itself and not by a GSH catabolite. Fast correction of GSH levels also indicates a fast turnover rate of GSH.

GSH toxic levels cause both potent UPR and a full iron starvation-like response

To search for causes of GSH toxicity, we established the mRNA profiles of HGT1 cells cultured with 50 μM GSH during 5, 30 and 240 min. The 5- and 30-min transcript profiles had similarities, but were distinct from the 4-h transcript profile that was not further considered as reflecting a non-specific stress response (Supplementary Figure S2). The 5-min response was modest (70 genes, Supplementary Table S1), and its significance was best appreciated in view of the 30-min response that was concurrent to the GSH peak. The 30-min response was large (375 genes, Supplementary Table S2) and included ∼50% of the genes regulated at 5 min (Supplementary Figure S3). Functional clustering revealed two major components in this response (Figure 2). The first one was highly similar to the response of iron-starved cells (Shakoury-Elizeh *et al*, 2004; Puig *et al*, 2005), and even more similar to that of the *atm1*Δ mutant (Hausmann *et al*, 2008). *ATM1* encodes a mitochondrial inner-membrane ABC transporter required for extra-mitochondrial ISC assembly (Hausmann *et al*, 2008). The HGT1 cell iron response comprised 25 genes of the iron regulon (Supplementary Table S2; Yun *et al*, 2000; Foury and Talibi, 2001; Rutherford *et al*, 2003) controlled by the Aft1 and Aft2 transcription factors, which regulates the uptake, compartmentalization and use of iron. Many repressed genes identified as part of the iron starvation response were also present here. These included genes encoding Fe–S- and haeme-containing proteins of mitochondrial respiration and the tricarboxylic acid cycle and of other pathways, and haeme, ergosterol, biotin and amino-acid/nitrogen biosynthetic enzymes. The second major component of the response to high GSH levels (115 genes, ∼30%) was a typical unfolded protein response (UPR) that is regulated by the Ire1 kinase and Hac1 transcription factor (Figure 2; Supplementary Table S2). It encompassed all major UPR gene categories induced by the model ER stress agents DTT and tunicamycin (Travers *et al*, 2000; Supplementary Figure S4A and B). Induction of several cytoplasmic chaperone genes could also be considered as satellite of the UPR, as the encoded proteins are known to help cells cope with ER stress (Liu and Chang, 2008). Repression of membrane proteins and proteins involved in ribosome biogenesis and translation might also be considered as part of the ER stress response, as shown in *C. albicans* (Wimalasena *et al*, 2008).

The UPR and iron starvation-like responses were independent of each other, as the latter persisted in HGT1 *ire1*Δ cells that had otherwise lost the UPR (Supplementary Figure S4C and D), but their concurrence probably caused conflicting gene regulation. For instance, haeme and ergosterol biosynthesis genes that are found repressed here are upregulated during the UPR.

GSH toxic levels inhibit cytoplasmic Fe–S maturation and activate Aft1

We explored the link between toxic GSH levels and iron metabolism. Addition of 100 μM GSH to HGT1 cells induced the Aft1 target-gene *FET3*, which peaked between 30 and 60 min (Figure 3A), confirming the microarray data. *FET3* was maximally induced at concentrations of GSH as low as 10 μM (Figure 3B). Aft1p is cytoplasmic in iron-replete cells, and accumulates in the nucleus in iron-deprived cells (Yamaguchi-Iwai *et al*, 2002). In accordance with *FET3* expression, in HGT1 cells, GFP-Aft1 became nuclear from a diffuse cellular pattern 15 min after addition of GSH (Figure 3C), and at concentrations of 10 μM and above (Supplementary Figure S5A). Although Aft1 was activated, iron was not limiting, as GSH-grown HGT1 cells had a slightly higher iron content than wild-type cells (Supplementary Figure S5B), and excess iron >100 μM worsened GSH toxicity (Figure 3D). Reciprocally, inactivating high-affinity iron uptake by deletion of *FET3*, which encodes the iron oxidase of the high-affinity iron uptake system, or *AFT1*, or *AFT1* and *AFT2* did not decrease GSH toxicity (Supplementary Figure S5C). Aft1 senses iron through the activity of mitochondrial ISC assembly (Chen *et al*, 2004) and mitochondrial ISC export systems, which are also required for extra-mitochondrial Fe–S protein assembly (Rutherford *et al*, 2005). In HGT1 cells, the activity of the mitochondrial Fe–S enzyme aconitase (Aco1) was not altered by GSH addition, in contrast to that of the cytoplasmic Fe–S enzyme isopropylmalate isomerase (Leu1), which decreased with a kinetics that inversely paralleled the GSH level changes (Figure 3E; see Figure 1D). Aco1 and Leu1 protein levels remained unchanged under all conditions (Figure 3F).

GSH toxic levels thus promptly trigger Aft1 activation and alter extra-mitochondrial but not mitochondrial Fe–S enzyme activity, both events occurring with time courses suggestive of a cause-and-effect relationship. Such alteration in iron metabolism may contribute to the lethality of high GSH levels, as several Fe–S proteins are essential.

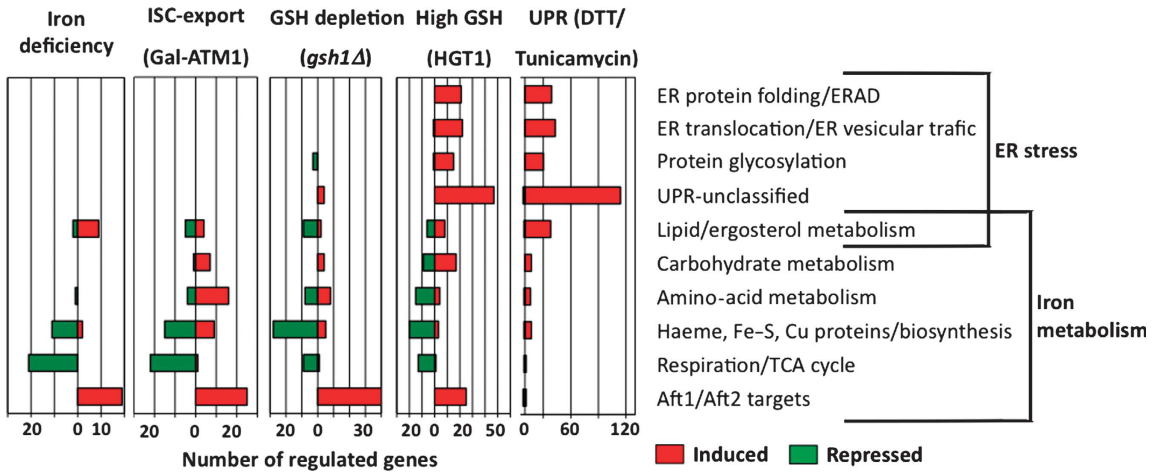

Figure 2 Synthetic view of genome-wide mRNA profile changes induced by toxic GSH levels and GSH depletion. Genes affected by GSH at toxic levels (HGT1 cells cultured with 50 μM GSH during 30 min), and by GSH depletion (*gsh1*Δ cells grown for three and six divisions in medium devoid of GSH) identified by DNA microarray analysis (see Supplementary Tables S2 and S3), in duplicate independent cultures, and assigned to functional categories (http://www.yeastgenome.org/cgi-bin/GO/goSlimMapper.pl). Numbers indicate the sum of regulated genes in each functional category. Genes represented comprise 61% (228/375) of the total genes regulated by GSH toxic levels and 68% (121/178) of the total genes regulated by GSH depletion. A few genes are present in more than one category. Data of transcriptional responses to *ATM1* depletion (Gal-*ATM1*) were from Hausmann *et al* (2008), to iron deficiency from Puig *et al* (2005) and to DTT/tunicamycin (UPR) from Travers *et al* (2000) and Kimata *et al* (2006).

High GSH levels cause an UPR by inhibiting ER oxidative protein folding

We explored the link between GSH toxic levels and the UPR. In HGT1 cells, the Hac1 target-gene *Kar2* was induced 5 min after GSH addition (Figure 4A), confirming the microarray data. Induction initially paralleled the increase in GSH levels, but then remained high for up to 4 h while GSH levels had corrected (see Figure 1D). *KAR2* induction occurred at GSH concentrations as low as 5 μM and reached a plateau at 50 μM (Figure 4B). As a thiol reductant, GSH might have induced the UPR by interfering with oxidative protein folding. We explored the impact of GSH on the Ero1 and Pdi1 redox states. In untreated HGT1 cells, Ero1 was fully oxidized and Pdi1 was almost fully oxidized. Addition of GSH caused a dose-dependent reduction of these proteins with a kinetics that paralleled the UPR, occurring fast and lasting for up to 1–3 h after GSH levels had corrected, depending on the GSH amount added (Figure 4C and D). Such kinetics suggested that GSH rapidly diffused into the ER and was trapped there, perpetuating Ero1 cycling by concomitantly reducing its negative regulatory disulphide and providing an unlimited reduced substrate supply. The presence of an actively cycling Ero1 was reflected by the GSH-dependent increase in the rate of GSH oxidation (Figure 4E), and by production of ROS (Figure 4F, upper) that are expected to be generated on reduction of oxygen by active Ero1 (Gross *et al*, 2006). An hour exposure of HGT1 cells to 100 μM GSH caused the ROS-specific probe rhodamine to fluoresce with a signal comparable to that produced by a 15-min exposure to 400 μM H_2O_2. The nature of this ROS signal was H_2O_2, as it was detected by the H_2O_2-specific PF1 probe (Supplementary Figure S6A), and its cellular origin the ER, as suggested its disappearance upon UPR prevention by Ire1 kinase inactivation (Figure 4F, lower). A further indication of Ero1-active cycling was the full reduction of Ero1, but not of Pdi1 (see Figure 4C and D), which indicated a balance between Ero1-mediated Pdi1 oxidation and its reduction by GSH. An active Ero1 was needed to counter the GSH-reductive load as HGT1 cells carrying the Ero1-defective *ero1-1* allele was intolerant to very low GSH concentrations (Supplementary Figure S6B).

We tested the effect of GSH on ER secretory transport by following the maturation of carboxypeptidase Y (Cpy), a protein requiring five disulphides for proper folding and ER to vacuole transport (Figure 4G). In HGT1 cells, a subtoxic concentration of GSH (20 μM) delayed Cpy maturation and a toxic one (50 μM) totally blocked this process, with accumulation of the ER form (p) and lack of appearance of the matured vacuolar form (m). The impact of GSH at 20 μM was equivalent to that of DTT at 5 mM, a dose–response difference that further supported the notion that GSH but not DTT accumulates into the ER at very high levels. Finally, inactivation of the UPR by *IRE1* deletion (*ire1*Δ) not only eliminated H_2O_2 production (see Figure 4F, lower), but also made HGT1 cells intolerant to very low and otherwise non-toxic GSH concentrations (Figure 4H; Supplementary Figure S6C). The latter data indicate that the impact of toxic levels of GSH on ER secretion contributes to its lethality, and that this lethality is not caused by the H_2O_2 produced in this condition.

Alteration of iron metabolism is the pre-eminent defect caused by GSH depletion

When grown in medium devoid of GSH, yeast cells lacking *GSH1* (*gsh1*Δ) become growth arrested after 8–10 divisions by near-complete GSH depletion (Spector *et al*, 2001); they activate Aft1 and are defective in extra-mitochondrial but not mitochondrial ISC maturation (Sipos *et al*, 2002; Rutherford *et al*, 2005; Figure 5A and C; Supplementary Figure S7A). However, it is not clear whether it is this defect or a defect in thiol-redox control that causes cell inviability by GSH depletion. To answer this question, we established the transcript profiles of *gsh1*Δ cells withdrawn of GSH for three or six divisions, the latter sample having extremely low GSH cellular levels (60 μM ~ 0.8% of WT) (Table I). The two GSH-depleted samples had almost identical mRNA profiles

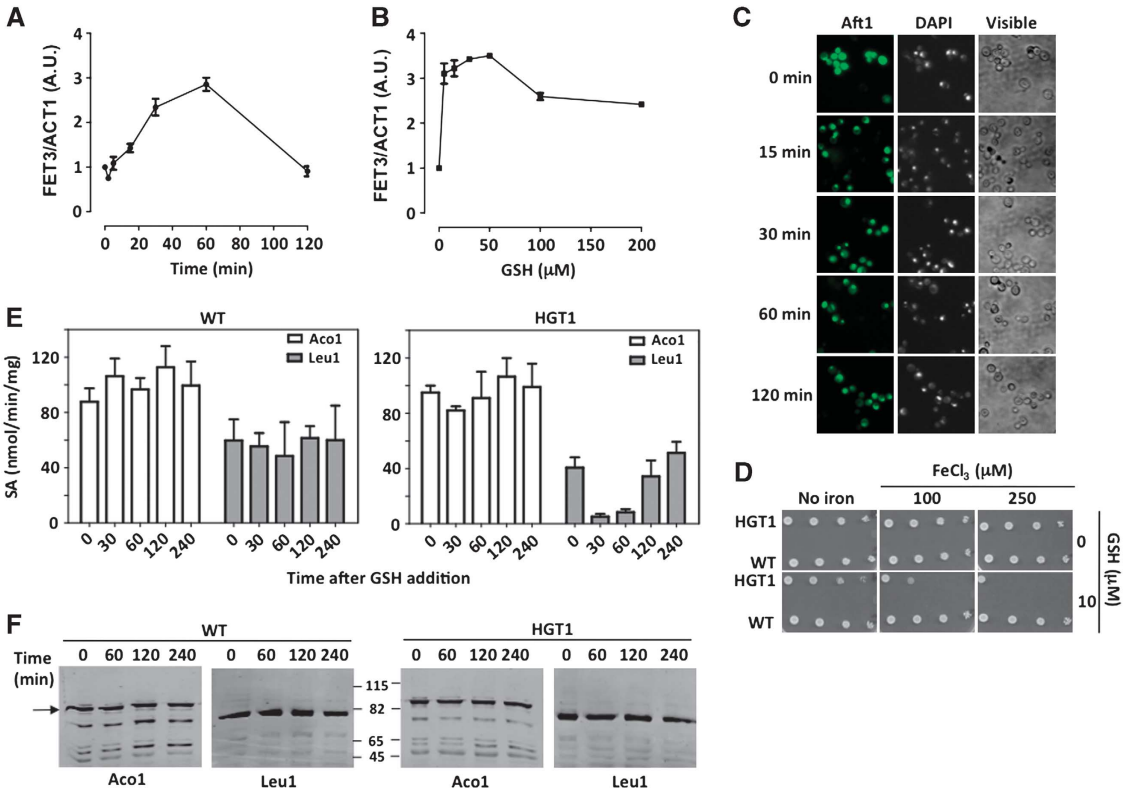

Figure 3 GSH toxic levels activate Aft1 and inhibit cytoplasmic Fe–S maturation. (**A**) *FET3* expression measured by RT–PCR in HGT1 cells at the indicated time after GSH addition (100 μM), or (**B**) 30 min after adding the indicated amount of GSH. *FET3* expression is given as *FET3/ACT1* signal ratio. Values are the mean of triplicate samples of the same experiment ± s.d. (**C**) GSH (50 μM) added to wild-type cells co-expressing pRS314-*TEF-HGT1* and p*TEF-AFT1-GFP*, and cellular GFP staining examined at the indicated time (left panel). DAPI nuclear staining (middle panel); visible-light image (right panel). (**D**) HGT1 and WT cells serially diluted and spotted onto SD plates containing no GSH, or 10 μM GSH, and/or no $FeCl_3$, or 100 or 250 μM $FeCl_3$. (**E**) GSH (100 μM) added to HGT1 or WT cells and Aco1 and Leu1 enzyme activities measured at the indicated time. Results are in specific activity (SA) (nM/min/mg protein). Data are the average of three independent experiments; error bars represent mean values ± s.d. (**F**) Extracts from the cells used in (**E**) were processed for western blot with anti-Aco1 or -Leu1 antibodies.

(Supplementary Figure S2), and were thus analysed as replicates of the same experiment. The observed response was significant (178 genes), and highly similar to that of the *atm1* mutant (Hausmann *et al*, 2008; Figure 2; Supplementary Table S3). In fact, with few exceptions, most genes responding to GSH depletion were categorized as part of an iron starvation-like response. A few gene targets of the H_2O_2-reponsive Yap1 transcription factor were also moderately induced, as noticed elsewhere (Wheeler *et al*, 2003), but their very limited number, several of which are in fact also controlled by Aft1 (see Supplementary Table S3), and lack of perceptible Yap1 oxidative activation (Figure 5B) indicate at best a very minor activation of Yap1. Interestingly, *HGT1* was also induced, which fulfilled the demand for increased GSH uptake.

The iron starvation-like response as the only significant genome-wide consequence of GSH depletion did not befit ascribing a thiol-redox control function at the origin of the GSH requirement for viability, which was previously established by the partial growth rescue of GSH-depleted cells by DTT (Sipos *et al*, 2002). We enquired of the effects of iron on GSH-depleted cells. Ferric iron (100 μM) partially decreased the high *FET3* expression of GSH-depleted cells within 15 min, while GSH totally corrected it (Figure 5C). As decrease in *FET3* mRNA levels by iron might reflect mRNA degradation rather than ISC assembly remediation (Hassett *et al*, 1998), we also inspected Leu1 activity (Figure 5D). A 1-h exposure of six-division GSH-depleted cells to $FeCl_3$ (300 μM) increased Leu1 activity from levels that were undetectable to more than half of those that were reached on a 1-h exposure to 1 μM GSH. Ferric iron (100 μM) also enabled some growth of *gsh1*Δ cells on medium lacking GSH, under anaerobiosis slightly better than aerobiosis (Supplementary Figure S7B). Iron can boost the loss of mitochondrial DNA (mtDNA) occurring during GSH depletion (Kistler *et al*, 1986; Ayer *et al*, 2010). We thus also tested its effect on a fully homogeneous petite *gsh1*Δ cell population, assuming that any adverse influence of iron on growth rate by mtDNA loss would be avoided. Growth of GSH-depleted petite *gsh1*Δ cells was now better rescued by ferric iron, irrespective of the presence of ambient oxygen, and with a dose-dependent effect up to 500 μM (Figure 5E and F). In comparison, growth rescue by DTT (1 mM) was smaller and was observed with cells less depleted of GSH (Figure 5F). Similar to DTT-rescued cells (Sharma *et al*, 2000; Spector *et al*, 2001), iron-rescued ones did not grow upon re-inoculation on medium containing iron but not GSH, indicating only transient, partial rescue.

Thus, the intense iron starvation-like response constituting the only significant genome-wide alteration of GSH-depleted cells suggests that it is a defect in iron metabolism that causes

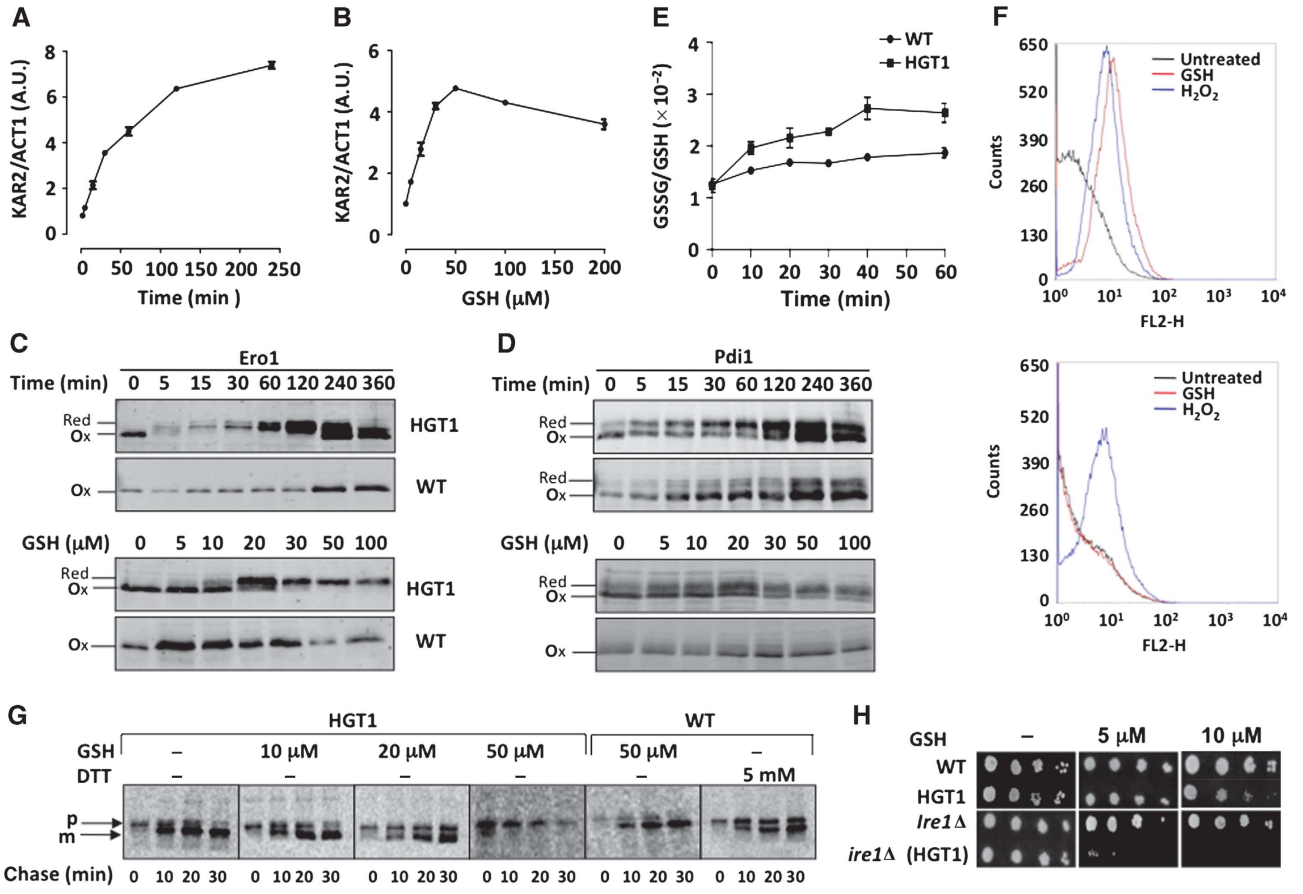

Figure 4 GSH toxic levels block secretion by ER reductive load. *KAR2* expression monitored by RT–PCR as in Figure 3A in (**A**) exponentially growing HGT1 cells at the indicated time after adding 100 μM GSH or (**B**) 30 min after adding the indicated amount of GSH (μM). *FET3* expression is given as *FET3*/*ACT1* signal ratio. Values are the mean of triplicate samples of the same experiment ± s.d. (**C**) HGT1 or WT cells expressing Myc-tagged Ero1 exposed to 50 μM GSH for the indicated time (upper panel) or for 30 min with the indicated amount of GSH (lower panel), and processed for redox western with anti-Myc antibodies. (**D**) As in (**C**), except that the western blot revealed with Pdi1-specific antibodies. (**E**) Fifteen minutes after adding GSH (50 μM) to HGT1 or WT cell cultures, 25 mM DTT was added. After 15 min, cells were collected, washed and inoculated in fresh SD medium at the same OD. Samples were collected for GSH and GSSG measurements. Data are the mean of three independent experiments ± s.d. (**F**) HGT1 (upper panel) or *ire1*Δ cells carrying HGT1 (lower panel) incubated for 1 h into PBS containing dihydrorhodamine 123 and either GSH (100 μM) or H_2O_2 (400 μM), or left untreated, and analysed by flow cytometry. Data are typical of three independent experiments. (**G**) HGT1 and WT cells incubated during 30 min with the indicated amount of GSH, pulsed with ^{35}S-methionine for 7 min and chased. Cpy was immunoprecipitated from cells collected at 0, 10, 20 and 30 min after chase initiation, separated by SDS–PAGE and revealed by phosphor technology. Arrows indicate Cpy immature (p) and mature vacuolar (m) forms. In last panel, WT cells treated with 5 mM DTT for 15 min, and processed, as above. (**H**) Exponentially growing WT or *ire1*Δ cells carrying pTEF-416-*HGT1* or empty vector serially diluted and spotted onto SD plates containing the indicated amount of GSH.

the inviability of these cells. The partial correction by iron of the ISC assembly and growth defects of these cells supports this conclusion.

GSH serves as backup of thioredoxin in thiol-redox maintenance

So far, by highlighting its role in iron metabolism while minimizing its impact on thiol-redox control, except for the high GSH levels on the ER, all data that were presented questioned the notion of the primary role of GSH in reducing oxidized Cys residues. Previous studies indicated a quasi-exclusive role of the thioredoxin pathway in peroxide metabolism (Le Moan *et al*, 2006), and a dominant role in RNR reduction (Camier *et al*, 2007). As another way to evaluate the actual GSH contribution to thiol-redox control, we evaluated how GSH coped with the redox load increase resulting from inactivation of thioredoxin reductase (*trr1*Δ). This strain carries a 1.5- to 3-fold increase in total GSH, with proportional increase of GSH and GSSG (Trotter and Grant, 2003; see Table I), presumably indicating a compensatory response to an increased redox load. In medium lacking GSH, *trr1*Δ cells grew very poorly. Adding high GSH amounts (100–200 μM) improved growth to near wild-type levels (Figure 6A), indicating that the redox peptide was still very limiting despite its 1.5- to 3-fold increase. To rigorously quantify the GSH demand caused by thioredoxin inactivation, we compared the *gsh1*Δ strain with a strain lacking both *GSH1* and *TRR1* (*gsh1*Δ*trr1*Δ). While the former strain only required 0.5 μM GSH to achieve a wild-type growth, the latter required 400-fold more GSH (200 μM) (Figure 6A). Anaerobiosis did not change the *gsh1*Δ GSH optimal growth requirement, but totally corrected the *trr1*Δ one (Figure 6B). Growth of the *gsh1*Δ*trr1*Δ strain was also improved, as now requiring 20-fold less GSH (10 versus 200 μM) for optimal growth (compare Figure 6A and B). However, such GSH requirement was still 20-fold higher than that of *gsh1*Δ (10 versus 0.5 μM), which indicated that an increased cellular redox load was still present in anaerobically grown *trr1*Δ. In *trr1*Δ, as

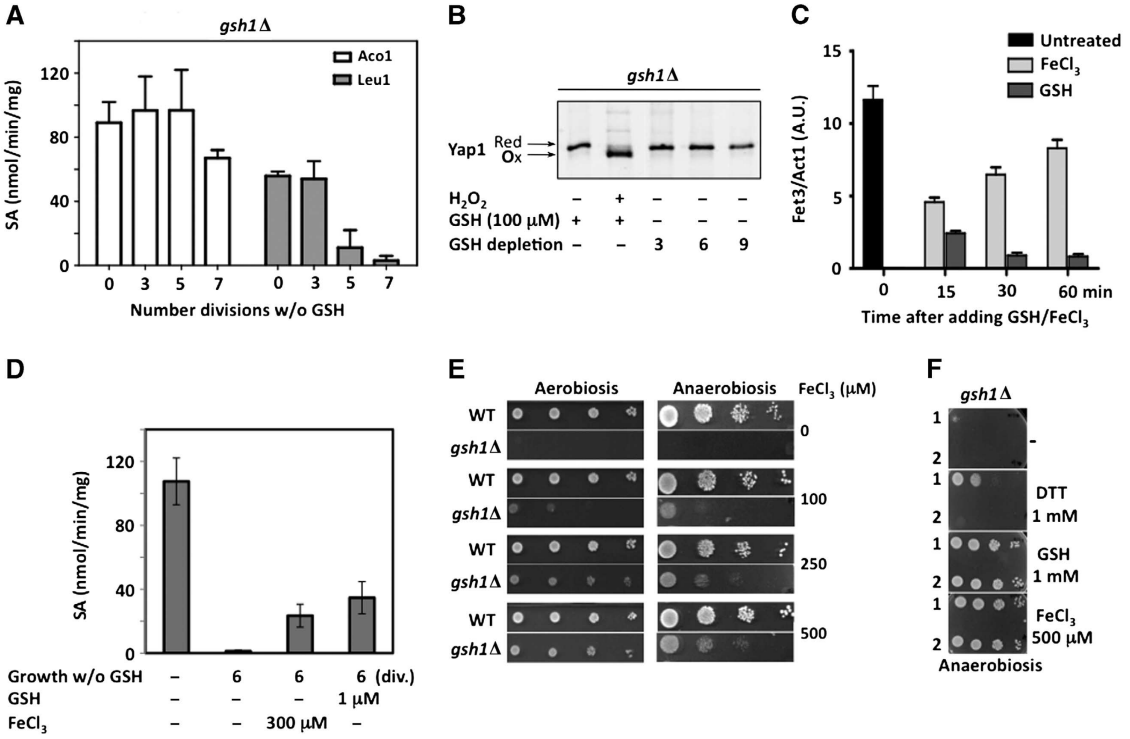

Figure 5 The effect of iron on GSH-depleted cells. (**A**) YPD-grown *gsh1*Δ cells inoculated in SD medium lacking GSH, grown for the indicated number of divisions, and processed for Aco1 and Leu1 enzyme activities. Data are the mean of three independent cultures ± s.d. (**B**) Same as in (**A**) with *gsh1*Δ cells carrying Myc–Yap1, and processed for redox western, using an anti-Myc antibody. (**C**) YPD-grown *gsh1*Δ cells inoculated in SD medium lacking GSH and grown for six divisions, and left untreated (black bar), or further incubated with GSH (1 mM) (dark grey bars) or $FeCl_3$ (100 μM) (light grey bars) for the indicated time (min). *FET3* expression monitored by RT–PCR as in Figure 3A. Values are the mean of triplicate samples of the same experiment ± s.d. (**D**) YPD-grown *gsh1*Δ cells re-inoculated in SD medium containing GSH (1 mM) or lacking GSH as indicated, were grown for six divisions, further incubated for 1 h with $FeCl_3$ (300 μM) or GSH (1 μM) and processed for Leu1 enzyme activity. Results are the mean ± s.d. of data from three independent cell cultures. (**E**) Wild-type (WT) and *gsh1*Δ petite (rho$^-$) cells (Y252 background) depleted of GSH by growth for six divisions in SD medium lacking GSH, serially diluted and spotted onto SD plates containing $FeCl_3$ (μM) at the indicated concentration, and incubated under aerobic (left panel) or anaerobic (right panel) conditions. (**F**) GSH non-depleted (grown overnight in SD medium with 1-mM GSH) (1) or depleted (grown for six division in SD medium lacking GSH) (2) *gsh1*Δ petite (rho$^-$) serially diluted and spotted onto SD plates containing DTT (1 mM), GSH (1 mM), $FeCl_3$ (500 μM) or nothing, and incubated under anaerobiosis.

in *gsh1*Δ*trr1*Δ, thioredoxin was largely oxidized (ox/red ~70%) compared with its oxidation in wild-type cells (~10%), and GSH addition decreased this oxidation back to 50% (Figure 6C) indicating that the extra-GSH improved the growth of these cells by balancing their redox load increase. Furthermore, note here (Figure 6C) that *trr1*Δ had more than a 10-fold increase in thioredoxin abundance, further demonstrating the tremendous compensatory response to an increased redox load. Conversely, however, in the absence of GSH, no increased redox load was applied on the thioredoxin pathway under aerobiosis, as indicated by total preservation of a wild-type redox state (ox/red ~10%) and levels of thioredoxin in *gsh1*Δ cells grown for up to 10 divisions in the absence of GSH (Figure 6D).

In summary, GSH is not capable on its own of efficiently bearing the redox load of the cell, whereas thioredoxin can do so without any increase in levels, which places GSH at best as backup of thioredoxin. As corollary, the contrast between the very high and trace amounts of GSH needed for thiol-redox maintenance and viability, respectively, should disqualify this function as explaining its viability requirement.

GSH links thiol-redox maintenance and iron metabolism

We enquired whether GSH linked thiol-redox and iron metabolism by monitoring *FET3* expression in thioredoxin reductase mutants. In *trr1*Δ, *FET3* had a 2.5-fold increased expression, but adding GSH returned this expression to wild-type levels (Figure 7A), which indicated that in these cells GSH is also limiting for iron metabolism despite its 1.5- to 3-fold compensatory increase in levels. In *gsh1*Δ*trr1*Δ, *FET3* expression was further induced, in keeping with the very low uncompensated GSH levels of these cells. Adding GSH decreased *FET3* expression, but only slightly and very transiently, as *FET3* mRNA levels increased again after 30 min (Figure 7B). The latter observation indicates that thioredoxin deficiency not only led to an increased GSH demand (see Figure 6A and B), but also caused very fast consumption of the redox peptide.

In conclusion, under conditions increasing its thiol-redox maintenance duties, GSH becomes limiting for its function in iron metabolism.

Discussion

We provide here data that question the view of glutathione as the major cellular redox buffer (Grant *et al*, 1999; Pocsi *et al*, 2004; Shelton and Mieyal, 2008), and emphasize the importance of its function in iron metabolism. We have analysed the genome-wide consequences of GSH depletion and its presence at toxic levels, using strains lacking *GSH1*

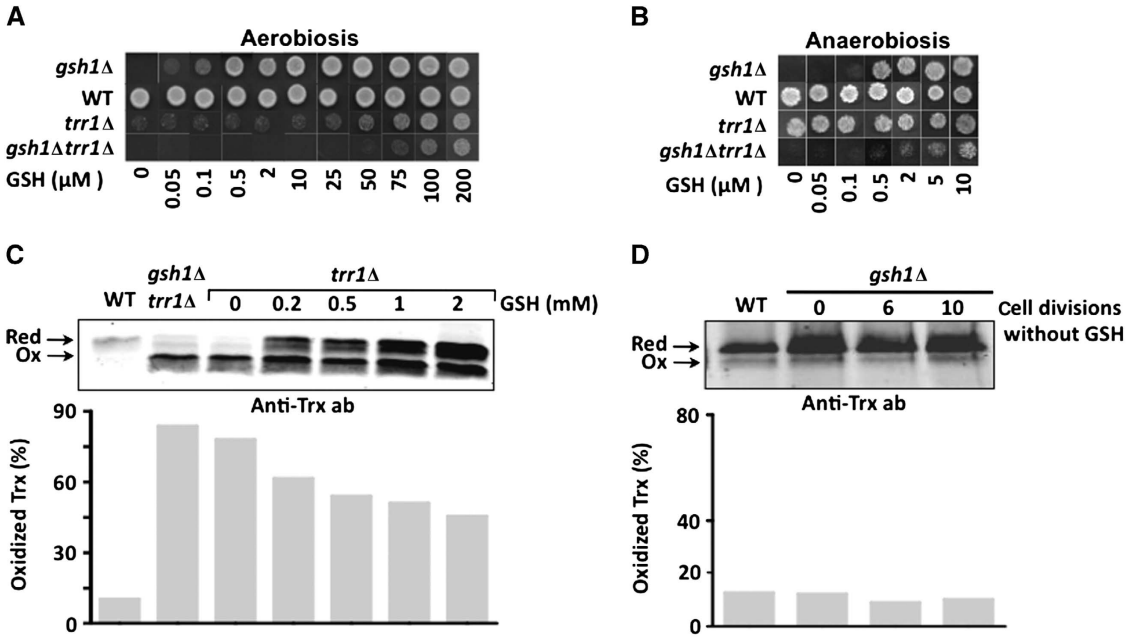

Figure 6 GSH serves as a backup of thioredoxin in thiol-redox maintenance. (**A**, **B**) *gsh1*Δ, WT, *trr1*Δ and *gsh1*Δ*trr1*Δ grown in SD medium lacking GSH to an $OD_{600} = 1$; a total of 2×10^6 cells of each culture were spotted onto SD plates containing the indicated amount of GSH (μM), and incubated under aerobic (**A**) or anaerobic conditions (**B**). Data are assembled from different plates. (**C**) WT, *gsh1*Δ*trr1*Δ and *trr1*Δ grown in SD medium lacking GSH, incubated for 1 h in SD medium containing or not containing GSH at the indicated concentration (mM) and processed for redox western with a thioredoxin-specific antibody. For WT cells, 2.5-fold more lysates were loaded. Arrows indicate oxidized (Ox) and reduced (Red) forms of thioredoxin. Lower panel: quantification of oxidized thioredoxin (%). (**D**) Same as in (**C**) with WT and *gsh1*Δ cells grown to saturation in YPD medium, re-inoculated in SD medium lacking GSH and allowed to grow for the indicated number of cell divisions.

or overexpressing the GSH-specific HGT1 transporter. Both lethal conditions trigger an intense iron starvation-like response associated with extra-mitochondrial Fe–S enzyme inactivation. Surprisingly, however, none of them impact thiol-redox metabolism, except for the effect of high GSH levels that impair ER oxidative protein folding and trigger the UPR as a vital adaptive measure. We also show, by evaluating the cellular redox load when thioredoxin is absent and conversely, that GSH is not capable of efficiently supporting the thiol-redox duties of the cell, despite a significant increase in its cellular levels, while thioredoxin can. We also contrast the high GSH demand for thiol-redox maintenance with the limited amount of it needed for viability, and show that iron can partially rescue the ISC maturation and growth defects of GSH-depleted cells. We propose that GSH is split between a function in iron metabolism that is vital, but only requires trace amounts of the redox peptide, and a thiol-redox maintenance function that serves as backup of the thioredoxin pathway, but requires much higher levels of the tripeptide (Figure 7C). A conflict between these two functions occurs under redox stresses that consume GSH, which activate Aft1 and may endanger cytoplasmic Fe–S protein maturation. Accordingly, the high GSH physiological levels in the mM range may not be meant for it to function as a cytosolic thiol-redox buffer, but to insulate its essential function in iron metabolism from variations of its concentration during redox stresses.

The redox-independent function of GSH in iron metabolism

Links between GSH and iron metabolism were initially suggested by the presence of increased and decreased levels of the tripeptide in yeast *ATM1* (Kispal *et al*, 1997) and frataxin mutants (Auchere *et al*, 2008), respectively. The observations that GSH depletion causes impairment of extra-mitochondrial ISC maturation (Sipos *et al*, 2002) and activates Aft1 (Rutherford *et al*, 2005), allowed identifying GSH as part of mitochondrial ISC export, a system providing to the CIA machinery a compound of undefined nature emanating from the mitochondrial ISC machinery (Lill, 2009), also serving as a signal that negatively regulates Aft1/2 (Chen *et al*, 2004). We now show that the near-unique genome-wide consequence of GSH depletion is a major iron starvation-like response remodelling most of iron-dependent mitochondrial and extra-mitochondrial pathways (see Figure 2). We also show that, unexpectedly, toxic GSH levels recapitulate the iron phenotype of GSH depletion. The molecular function of GSH in iron metabolism may not involve a conventional thiol-disulphide reductase activity, as suggests the ability of iron (Figure 5D), but not DTT (Sipos *et al*, 2002), to partially correct the ISC defect of GSH-depleted cells. GSH probably engages a partnership with Grx3 and Grx4, with which it forms *in vitro* unusual Fe–S-bridged dimeric complexes that are coordinated by its Cys residue and the glutaredoxin active site ones (Li *et al*, 2009; Rouhier *et al*, 2009). A recent report has provided proofs of the *in vivo* presence of these unusual Fe–S clusters, and has proposed that they deliver iron to all iron-containing proteins and to mitochondria (Muhlenhoff *et al*, 2010). The slightly higher GSH requirement of cells lacking *GSH1, GRX3* and *GRX4* in comparison with those only lacking *GSH1* (Supplementary Figure S7C) is tantamount of synthetic lethality, and indicate that the corresponding gene products operate in the same essential pathway. Nevertheless, the ability of iron to improve the ISC assembly defect of GSH-depleted cells could also indicate a specific function of GSH in cytosolic iron delivery. However, while

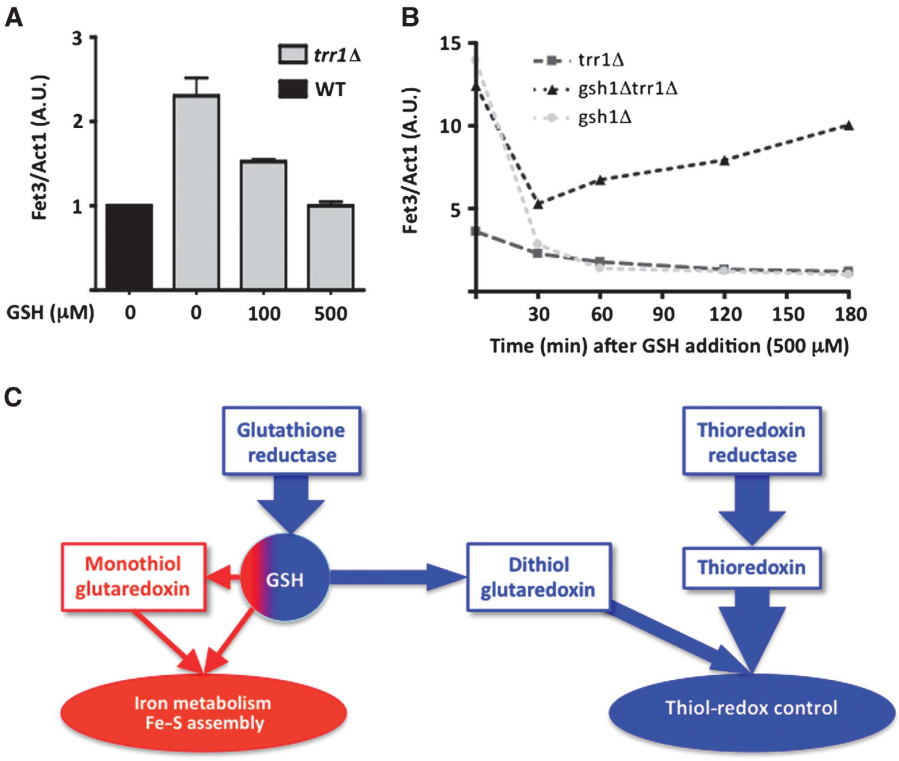

Figure 7 GSH establishes a functional crosstalk between iron metabolism and thiol-redox maintenance. (**A**) WT (black) and *trr1*Δ (light grey) grown in SD medium lacking GSH, re-inoculated in SD medium containing the indicated amount of GSH and allowed to grow for 1 h. *FET3* expression measured by RT–PCR as in Figure 3A. Values are the mean of triplicate samples of the same experiment ± s.d. (**B**) *trr1*Δ (dark grey square), *gsh1*Δ*trr1*Δ (black triangle) and *gsh1*Δ (light grey circle) grown in SD medium lacking GSH until GSH depletion, at which time GSH (500 μM) was added; cells were further incubated for the indicated time (min) and processed for *FET3* expression as in (**A**). Values are the mean of triplicate samples of the same experiment ± s.d. (**C**) Schematics of the GSH physiological role split between an iron function, which is vital but only requires trace amounts of the tripeptide, and a thiol-redox maintenance function, which appears as a backup of the thioredoxin pathway but requires much higher levels of the tripeptide. In the absence of thioredoxin reductase, GSH takes up on thiol-redox maintenance duties and thus becomes limiting for its vital iron function.

Grx3/4 depletion inactivates both mitochondrial and extra-mitochondrial ISC assembly (Ojeda *et al*, 2006; Muhlenhoff *et al*, 2010), GSH depletion only inactivates the latter (Sipos *et al*, 2002) (this study), which does not fit the notion of shared functions of GSH and Grx3/4, by Fe–S cluster coordination. These seeming discrepancies might be, at least in part, linked to the incomplete nature of GSH cellular depletion that causes cell death by affecting first extra-mitochondrial ISC assembly before the full phenotypic scope of GSH deficiency reveals, which could also suggest wider functions of GSH in iron metabolism than Grx3/4.

Toxic GSH levels also impaired Leu1 activity, while sparing Aco1 activity. Impairment of the cytosolic Fe–S enzymes could be caused by disruption of the Grx3/4-GSH Fe–S clusters by titration of Grxs by GSH; however, overexpressing Grx4 in HGT1 cells only corrected GSH-induced high *FET3* expression but not growth inhibition (Supplementary Figure S5D, E and F). High GSH levels could also prevent formation of the GSH-Grx3/4 Fe–S clusters by iron sequestration, or could directly affect cytosolic Fe–S enzymes, as suggests the very fast inhibition of Leu1 (see Figure 3). The fact that toxic GSH levels spared mitochondrial iron metabolism was surprising, and might relate to the exclusion from this organelle of the high GSH levels reached in HGT1 cells (not shown). Further work will be needed to establish the molecular function and toxicity of GSH in iron metabolism and its partnership with Grx3/4.

The redox impact of glutathione

The data presented here, all point to a limited cytosolic redox function of GSH. GSH depletion should have caused Cys residue oxidation, but the genome-wide mRNA profiles of GSH-depleted cells did not reveal any other hint of redox imbalance than induction of a very few Yap1 targets (see Figure 2; Supplementary Table S3). This result, and the observation that GSH depletion does not cause any proteome-wide thiol oxidation (Le Moan *et al*, 2006), suggest that GSH is totally dispensable for cytosolic thiol-redox maintenance. Reciprocally high GSH levels should have caused Cys residue reduction, but this effect was only observed in the ER, in which GSH led to total reduction of Ero1 and Pdi1, which blocked secretion and induced the UPR (see Figure 4). We also show, using cells with inactivation of the thioredoxin pathway, that GSH is not capable of supporting the redox load of the cell on its own. Despite the presence of a 1.5- to 3-fold compensatory increase of total GSH in *trr1*Δ (Trotter and Grant, 2003; see Table I), the redox peptide was still very limiting for growth (Figure 6A) and was unable to sustain the redox load increase resulting from the lack of thioredoxin reductase. A large part of the redox load

increase in *trr1*Δ was linked to aerobic metabolism, but was also present under anaerobiosis (Figure 6A and B). Reciprocally, cells that were severely depleted of GSH preserved thioredoxin in their wild-type redox state, without any protein compensatory increase, indicating that the thioredoxin pathway could entirely assume the thiol-redox maintenance duties of the cell. These observations and the quasi-exclusive role of the thioredoxin pathway in peroxide metabolism (Le Moan *et al*, 2006) and a dominant role in RNR reduction (Camier *et al*, 2007), place GSH as an ancillary system of the thioredoxin pathway in cytosolic thiol-redox control.

The bases of the essential nature and toxicity of GSH

The GSH requirement for viability could theoretically be linked to either its thiol-redox or iron-metabolism functions, as both these processes are essential (Toledano *et al*, 2007; Lill, 2009). Notwithstanding, the notion that GSH thiol-redox maintenance only serves as backup of thioredoxin, disqualifies this function as causing the GSH essential requirement. The contrast between the very high GSH levels needed for thiol-redox maintenance in the absence of thioredoxin and the very low intracellular GSH levels required for viability (Figure 6A; Table I), at which GSH should behave as a thiol oxidant, further support this idea. Still, GSH could have one exclusive essential redox target, but this is unlikely, as DTT should have then totally rescued the growth of GSH-depleted cells, as it does in *E. coli* that is made unviable by inactivation of thioredoxin reductase and glutathione reductase (Ortenberg *et al*, 2004; Gon *et al*, 2006a). Contrasting with the negligible importance of its thiol-redox function, the function of GSH in iron metabolism appeared pre-eminent. The intense iron starvation-like response that constituted the near-unique genome-wide consequence of GSH depletion befit the idea that it is this function that makes GSH essential, which is supported by the partial rescue by iron of the ISC and growth defects of GSH-depleted cells. DTT can also partially rescue GSH auxotrophy (Grant *et al*, 1996; see Figure 5F), presumably by substituting for some of its redox functions, thereby decreasing its consumption (Sharma *et al*, 2000; Spector *et al*, 2001; Ayer *et al*, 2010), or by recruiting GSH by reduction of GSSG, thus temporarily sparing its vital iron function.

The lethal effect of toxic levels of GSH is clearly linked to its impact on secretion, as indicated by the partial growth rescue of HGT1 cells by the thiol oxidant diamide that decreased ER reductive stress (not shown), and by the much lower GSH tolerance of HGT1 *ire1*Δ. The latter observation also indicates that cell death caused by prolonged ER stress is not linked to H_2O_2 production (Haynes *et al*, 2004), as HGT1 *ire1*Δ cells did not generate H_2O_2 when exposed to GSH, but were much more sensitive to its toxicity. The GSH impact on iron metabolism may also affect viability, but how it does so will only be deduced from knowledge of its molecular function in this pathway.

Conclusions

The data presented here provide a framework of the cellular organization, compartmentation and functions of thiol-redox pathways in eukaryotic cells that has been lacking. They also establish an unsuspected crosstalk between thiol-redox and iron homeostasis that probably applies to higher eukaryotes, in which GSH is also essential for viability (Shi *et al*, 2000) and partners with glutaredoxins to assemble Fe–S clusters (Rouhier *et al*, 2009). Although higher eukaryotes have necessarily more complex thiol-redox systems, as here but not in yeast, GSH is also involved in peroxide scavenging by serving as exclusive proton donor for the peroxide scavengers glutathione peroxidases (Toledano *et al*, 2007), and by constituting a cellular nitric oxide storage in the form of nitrosoglutathione (GS-NO) (Hess *et al*, 2005). The redox-iron homeostasis crosstalk described here predicts a novel toxic mechanism for redox stresses caused by peroxides, electrophilic xenobiotics and metals that may endanger fitness not only by direct effect but by consumption of GSH and inhibition of cytoplasmic Fe–S protein maturation. Knowledge of such crosstalk should contribute to elucidating the intricate pathophysiological links between redox imbalance, GSH depletion, alterations of iron metabolism and oxidative stress underlying age-related diseases, such as neurodegeneration and inflammation (Altamura and Muckenthaler, 2009; Bharath *et al*, 2002; Lee *et al*, 2009).

Materials and methods

Yeast strains, growth conditions and plasmids

The *S. cerevisiae* strains ABC 1144 (WT) and ABC 1230 (HGT1 cells) are derived from YPH499 (MATα *ura3-52 leu2*Δ*-1 lys2-801 his3*Δ*-200 trp1-63 ade2-101*) and carry an integrated *URA3* cassette or TEF-*HGT1*, respectively (Srikanth *et al*, 2005). Y252, isogenic *gsh1*Δ (Spector *et al*, 2001) and *trr1*Δ (Le Moan *et al*, 2006) were described. The *gsh1*Δ*trr1*Δ strain was produced by integrating *KanMX4* at the *TRR1* locus in *gsh1*Δ. BY4742 and isogenic derivative *ire1*Δ are from EUROSCARF. The pTEF-416-*HGT1* plasmid (*CEN URA3 TEF-HGT1*) has been described (Bourbouloux *et al*, 2000); pRS314-*TEF-HGT1* (*CEN TRP1 TEF-HGT1*) was constructed by subcloning a partial SacI–KpnI digest fragment from pTEF416-*HGT1* into pRS314; p*AFT1-GFP* is a gift from MA de la Torres-Ruiz (Lleida, Spain) (Pujol-Carrion *et al*, 2006); p*TEF-AFT1-GFP* was constructed by inserting a pTEF-416 400-bp SacI–XbaI fragment containing the *TEF1* promoter in place of the *MET25* promoter in p*AFT1-GFP*; pAF85 (*CEN LEU2 ERO1–Myc*) is a gift from Chris Kaiser (Sevier *et al*, 2007). pRS316–Myc–Yap1 was described (Delaunay *et al*, 2002). Cells were grown in YPD (1% yeast extract, 2% peptone and 2% glucose), YPG (same as YPD, with 2% glycerol instead of glucose), or minimal media (SD) (0.67% yeast nitrogen base w/o amino acids, 2% glucose), or minimal media glycerol (SG) (same as SD with 2% glycerol instead of glucose) with amino-acid supplements as appropriate, at 30°C. Anaerobic growth was performed as described (Spector *et al*, 2001). For generating respiratory incompetent (petite) *gsh1*Δ, cells were grown overnight in YPD, and then diluted in SD without GSH until they were growth arrested, re-inoculated in SD + 100 μM GSH, and tested for their ability to grow on YPG. GSH, GSSG and ferric chloride ($FeCl_3$) were obtained from Sigma.

Measures of glutathione by LC-tandem MS

The pellet of cold H_2O-washed yeast cells was suspended in perchloric acid (0.1%, pH 2), boiled (95°C, 5 min) and centrifuged. An aliquot of the supernatant, which correspond to the metabolic fraction, was mixed with an aliquot of an ^{15}N-labelled reference metabolic fraction, and diluted with formic acid (0.1%) to reach the equivalent of 4×10^7 cells/ml, and injected into the chromatographic system for analysis, as described (Lafaye *et al*, 2005). GSH and GSSG concentrations in mM/cell were calculated on the basis of an average yeast cell volume of 4.5×10^{-14}l, which assumes that yeast cells are spherical, with an average diameter of 4.4 μM, as determined by microscopic measurement of 100 cells. We ensured that these size parameters did not change with strain backgrounds and growth conditions.

Microarray analysis

For each growth condition, microarray experiments were performed in two replicates with RNA isolated from independent cultures grown on different days. Each replicate comprised a dye swap

between the experimental and reference samples. Totals RNAs were extracted using the Agilent Total RNA isolation mini kit. Labelled complementary RNAs (cRNAs) were generated using the Agilent Low RNA Input Linear Amplification Kit. The cRNA synthesis and Cy-Dye incorporation efficacies were checked by spectrophotometry. Equal amounts of Cy3- (reference sample) and Cy5 (experimental sample)-labelled probes, and the reverse for the dye swap reaction, were mixed together and hybridized onto the Agilent Yeast Oligo Microarray (V2) slides. Slides were scanned using the GenePix 4000B scanner (Molecular Devices). Raw data of spot intensities corrected for background signals were calculated using GenePix Pro 6.0 (Molecular Devices) and exported to GeneSpring Gx 7.3 (Silicon genetics Agilent) for normalization and statistical analyses (see Supplementary data). Genes with an expression change of $\geqslant$2-fold were considered induced or repressed. A lower cutoff of $\geqslant$1.7-fold was used for the 5-min HGT1 condition.

Real-time quantitative PCR

Unique oligonucleotide primer pairs were designed with the QuantPrime software (http://www.quantprime.de) and assayed on efficiency (>80%) and specificity. Six micrograms of RNeasy Mini kit (Quiagen) purified total RNA, digested with RQ1 RNase-Free DNase (Promega) was reverse-transcribed with SuperScript II reverse transcriptase (Invitrogen) with random hexanucleotides (Roche Diagnostics). Real-time quantitative PCR was performed in triplicate as described (Desaint *et al*, 2004).

Fluorescence microscopy and flow cytometry

Aft1-GFP subcellular localization used cells carrying p*TEF-AFT1-GFP* stained with DAPI, washed, suspended into DABCO and visualized as described (Delaunay *et al*, 2002). For detection of H_2O_2, cells were collected, washed, incubated for 10 min in PBS containing Peroxyfluor-1 (PF1; 10 μM; a gift from Chris Chang, California, USA) (Miller *et al*, 2005), collected, washed, suspended into PBS containing the indicated amount of GSH or H_2O_2, and analysed by fluorescence microscopy. Alternatively, cells were collected and suspended into PBS containing the indicated amount of GSH and dihydrorhodamine 123 (20 μM) (Invitrogen), incubated for 1 h at 30°C, and analysed by flow cytometry as described (Desaint *et al*, 2004).

Leu1 and aconitase enzyme assays

The pellet of yeast cell cultures was suspended in lysis buffer (Tris–HCl (10 mM, pH 7.4), EDTA (2.5 mM), NaCl (150 mM), glycerol (10%, v/v) and Triton X-100 (0.5%, v/v)), and lysed by agitation with glass beads. Cell extracts were centrifuged and supernatants were used for enzyme assays. Aco1 activity was measured by the disappearance of cis-Aconitate at 240 nm, and Leu1 by the decrease in absorbance at 235 nm using citraconate as described (Kispal *et al*, 1999). Aco1 and Leu1 protein levels were quantified by western blot using polyclonal anti-Aco1, a gift from Anne Bulteau (Paris, France), and anti-Leu1, a gift from Rolland Lill (Marburg, Germany), antibodies. Total cellular iron was determined in mole/cell from a 250-ml culture of exponentially growing HGT1 cells ($OD_{600} = 0.3–0.4$) as described (Doeg and Ziegler, 1962).

Pulse-chase labelling and immunoprecipitation

Exponential phase cells were suspended in 10-ml SD medium lacking methionine ($\sim 6 \times 10^7$ cells/ml), pulse-labelled with 500 μCi of [^{35}S] methionine (NEN, Perkin-Elmer) for 7 min and chased with excess cold methionine. A volume of 1.5 ml samples (1×10^8 cells) were collected in 20 mM NaN_3, lysed in 100 μl of lysis buffer (Tris–HCl (50 mM, pH 7.5), EDTA (1 mM), sodium dodecyl sulphate (SDS; 1%), urea (6 M) protease inhibitor complete (Roche) (1 ×), PMSF (1 mM)) by agitation with glass beads, and by boiling. Cell extracts were suspended in 1 ml of IP buffer (Tris–HCl (50 mM, pH 7.5), NaCl (150 mM), EDTA (1 mM), Tween-20 (0.5%), protease inhibitor complete (1 ×) and PMSF (1 mM)), mixed with Sheep anti-Mouse IgG Dynabeads® (Invitrogen) coupled to mouse monoclonal anti-Cpy1 antibodies. The mix was tumbled for 2 h at 4°C, washed three times in IP buffer, recovered in 20 μl 1 × Laemmli buffer, boiled and separated by 8% SDS–PAGE. Gels were analysed with a Storm PhosphorImager and ImageQuant TL Software (GE Healthcare).

Redox western

Trichloroacetic acid-precipitated cell extracts (Delaunay *et al*, 2002) were dissolved in SB buffer (Tris–Cl (100 mM, pH 8.8), EDTA (10 mM) and SDS (1%)) containing 30 mM 4-acetamido-4′-maleimidylstilbene-2,2′-disulphonic acid (AMS, Invitrogen), or 50 mM N-ethylmaleimide and incubated at 37°C for 2 h. Protein concentration was measured by bicinchoninic acid-based colorimetric detection (micro BCA kit, Pierce). For Ero1 and Pdi1, 20 μg protein extracts were mixed with 3 × Laemmli buffer without β-mercaptoethanol, boiled and deglycosylated by incubation with 250 units of endoglycosidase H (NEB) for 60 min at 37°C after addition of sodium citrate (67 mM, pH 5.5). Proteins were resolved by non-reducing SDS–PAGE, and revealed by western blot with 9E10 anti-Myc monoclonal (a gift from C Créminon, Saclay, France), anti-Pdi1 rabbit polyclonal (a gift from J Winther, Denmark), rabbit polyclonal anti-thioredoxin (a gift from C Grant, UK) or anti-His antibodies, anti-mouse IgG or anti-rabbit IgG secondary antibodies labelled with fluorophores of different wavelengths, followed by Infrared Imaging technology (Odyssey, LI-COR).

Supplementary data

Supplementary data are available at *The EMBO Journal* Online (http://www.embojournal.org).

Acknowledgements

We thank F Tacnet for help with fluorescence microscopy and scientific discussions, and Marie-Elyse Lancelot for the microarray analysis. We acknowledge A Bulteau, C Chang, C Grant, C Kaiser, R Lill, MA de la Torres-Ruiz and J Winther for gifting reagents. This work was funded by grant from ANR SOLEMA to MBT, and from the Department of Biotechnology, government of India to AKB. MBT is the recipient of a programme grant from La Ligue Contre le Cancer (LNCC).

Author contributions: CK, AI and MBT planned the experiments; CK and AI performed most experiments; BD′A and AI the enzyme assays; BD′A the iron measurements; EG and CJ the GSH measurements and AGP the ROS measurements; AKB provided reagents; CK, AI, BD′A, ADM and MBT analysed the results; MBT wrote the manuscript.

Conflict of interest

The authors declare that they have no conflict of interest.

References

Altamura S, Muckenthaler MU (2009) Iron toxicity in diseases of aging: Alzheimer′s disease, Parkinson′s disease and atherosclerosis. *J Alzheimers Dis* **16:** 879–895

Auchere F, Santos R, Planamente S, Lesuisse E, Camadro JM (2008) Glutathione-dependent redox status of frataxin-deficient cells in a yeast model of Friedreich's ataxia. *Hum Mol Genet* **17:** 2790–2802

Ayer A, Tan SX, Grant CM, Meyer AJ, Dawes IW, Perrone GG (2010) The critical role of glutathione in maintenance of the mitochondrial genome. *Free Radic Biol Med* **49:** 1956–1968

Bharath S, Hsu M, Kaur D, Rajagopalan S, Andersen JK (2002) Glutathione, iron and Parkinson's disease. *Biochem Pharmacol* **64:** 1037–1048

Bourbouloux A, Shahi P, Chakladar A, Delrot S, Bachhawat AK (2000) Hgt1p, a high affinity glutathione transporter from the yeast Saccharomyces cerevisiae. *J Biol Chem* **275:** 13259–13265

Camier S, Ma E, Leroy C, Pruvost A, Toledano M, Marsolier-Kergoat MC (2007) Visualization of ribonucleotide reductase catalytic oxidation establishes thioredoxins as its major reductants in yeast. *Free Radic Biol Med* **42:** 1008–1016

Chen OS, Crisp RJ, Valachovic M, Bard M, Winge DR, Kaplan J (2004) Transcription of the yeast iron regulon does not respond directly to iron but rather to iron-sulfur cluster biosynthesis. *J Biol Chem* **279:** 29513–29518

Cuozzo JW, Kaiser CA (1999) Competition between glutathione and protein thiols for disulphide-bond formation. *Nat Cell Biol* **1:** 130–135

Delaunay A, Pflieger D, Barrault MB, Vinh J, Toledano MB (2002) A thiol peroxidase is an H2O2 receptor and redox-transducer in gene activation. *Cell* **111:** 471–481

Desaint S, Luriau S, Aude JC, Rousselet G, Toledano MB (2004) Mammalian antioxidant defenses are not inducible by H2O2. *J Biol Chem* **279:** 31157–31163

Doeg KA, Ziegler DM (1962) Simplified methods for the estimation of iron in mitochondria and submitochondrial fractions. *Arch Biochem Biophys* **97:** 37–40

Foury F, Talibi D (2001) Mitochondrial control of iron homeostasis. A genome wide analysis of gene expression in a yeast frataxin-deficient strain. *J Biol Chem* **276:** 7762–7768

Frand AR, Kaiser CA (1998) The ERO1 gene of yeast is required for oxidation of protein dithiols in the endoplasmic reticulum. *Mol Cell* **1:** 161–170

Ganguli D, Kumar C, Bachhawat AK (2007) The alternative pathway of glutathione degradation is mediated by a novel protein complex involving three new genes in Saccharomyces cerevisiae. *Genetics* **175:** 1137–1151

Gon S, Camara JE, Klungsoyr HK, Crooke E, Skarstad K, Beckwith J (2006a) A novel regulatory mechanism couples deoxyribonucleotide synthesis and DNA replication in Escherichia coli. *EMBO J* **25:** 1137–1147

Gon S, Faulkner MJ, Beckwith J (2006b) *In vivo* requirement for glutaredoxins and thioredoxins in the reduction of the ribonucleotide reductases of Escherichia coli. *Antioxid Redox Signal* **8:** 735–742

Grant CM, MacIver FH, Dawes IW (1996) Glutathione is an essential metabolite required for resistance to oxidative stress in the yeast Saccharomyces cerevisiae. *Curr Genet* **29:** 511–515

Grant CM, Quinn KA, Dawes IW (1999) Differential protein S-thiolation of glyceraldehyde-3-phosphate dehydrogenase isoenzymes influences sensitivity to oxidative stress. *Mol Cell Biol* **19:** 2650–2656

Gross E, Sevier CS, Heldman N, Vitu E, Bentzur M, Kaiser CA, Thorpe C, Fass D (2006) Generating disulfides enzymatically: reaction products and electron acceptors of the endoplasmic reticulum thiol oxidase Ero1p. *Proc Natl Acad Sci USA* **103:** 299–304

Hassett RF, Romeo AM, Kosman DJ (1998) Regulation of high affinity iron uptake in the yeast Saccharomyces cerevisiae. Role of dioxygen and Fe. *J Biol Chem* **273:** 7628–7636

Hausmann A, Samans B, Lill R, Muhlenhoff U (2008) Cellular and mitochondrial remodeling upon defects in iron-sulfur protein biogenesis. *J Biol Chem* **283:** 8318–8330

Haynes CM, Titus EA, Cooper AA (2004) Degradation of misfolded proteins prevents ER-derived oxidative stress and cell death. *Mol Cell* **15:** 767–776

Hess DT, Matsumoto A, Kim SO, Marshall HE, Stamler JS (2005) Protein S-nitrosylation: purview and parameters. *Nat Rev Mol Cell Biol* **6:** 150–166

Kaur H, Kumar C, Junot C, Toledano MB, Bachhawat AK (2009) Dug1p Is a Cys-Gly peptidase of the gamma-glutamyl cycle of Saccharomyces cerevisiae and represents a novel family of Cys-Gly peptidases. *J Biol Chem* **284:** 14493–14502

Kimata Y, Ishiwata-Kimata Y, Yamada S, Kohno K (2006) Yeast unfolded protein response pathway regulates expression of genes for anti-oxidative stress and for cell surface proteins. *Genes Cells* **11:** 59–69

Kispal G, Csere P, Guiard B, Lill R (1997) The ABC transporter Atm1p is required for mitochondrial iron homeostasis. *FEBS Lett* **418:** 346–350

Kispal G, Csere P, Prohl C, Lill R (1999) The mitochondrial proteins Atm1p and Nfs1p are essential for biogenesis of cytosolic Fe/S proteins. *EMBO J* **18:** 3981–3989

Kistler M, Summer KH, Eckardt F (1986) Isolation of glutathione-deficient mutants of the yeast Saccharomyces cerevisiae. *Mutat Res* **173:** 117–120

Lafaye A, Labarre J, Tabet JC, Ezan E, Junot C (2005) Liquid chromatography-mass spectrometry and 15N metabolic labeling for quantitative metabolic profiling. *Anal Chem* **77:** 2026–2033

Lange H, Lisowsky T, Gerber J, Muhlenhoff U, Kispal G, Lill R (2001) An essential function of the mitochondrial sulfhydryl oxidase Erv1p/ALR in the maturation of cytosolic Fe/S proteins. *EMBO Rep* **2:** 715–720

Le Moan N, Clement G, Le Maout S, Tacnet F, Toledano MB (2006) The Saccharomyces cerevisiae proteome of oxidized protein thiols: contrasted functions for the thioredoxin and glutathione pathways. *J Biol Chem* **281:** 10420–10430

Lee DW, Kaur D, Chinta SJ, Rajagopalan S, Andersen JK (2009) A disruption in iron-sulfur center biogenesis via inhibition of mitochondrial dithiol glutaredoxin 2 may contribute to mitochondrial and cellular iron dysregulation in mammalian glutathione-depleted dopaminergic cells: implications for Parkinson's disease. *Antioxid Redox Signal* **11:** 2083–2094

Li H, Mapolelo DT, Dingra NN, Naik SG, Lees NS, Hoffman BM, Riggs-Gelasco PJ, Huynh BH, Johnson MK, Outten CE (2009) The yeast iron regulatory proteins Grx3/4 and Fra2 form heterodimeric complexes containing a [2Fe-2S] cluster with cysteinyl and histidyl ligation. *Biochemistry* **48:** 9569–9581

Lill R (2009) Function and biogenesis of iron-sulphur proteins. *Nature* **460:** 831–838

Liu Y, Chang A (2008) Heat shock response relieves ER stress. *EMBO J* **27:** 1049–1059

Luikenhuis S, Perrone G, Dawes IW, Grant CM (1998) The yeast Saccharomyces cerevisiae contains two glutaredoxin genes that are required for protection against reactive oxygen species. *Mol Biol Cell* **9:** 1081–1091

Meister A, Anderson ME (1983) Glutathione. *Annu Rev Biochem* **52:** 711–760

Miller EW, Albers AE, Pralle A, Isacoff EY, Chang CJ (2005) Boronate-based fluorescent probes for imaging cellular hydrogen peroxide. *J Am Chem Soc* **127:** 16652–16659

Muhlenhoff U, Molik S, Godoy JR, Uzarska MA, Richter N, Seubert A, Zhang Y, Stubbe J, Pierrel F, Herrero E, Lillig CH, Lill R (2010) Cytosolic monothiol glutaredoxins function in intracellular iron sensing and trafficking via their bound iron-sulfur cluster. *Cell Metab* **12:** 373–385

Muller EG (1991) Thioredoxin deficiency in yeast prolongs S phase and shortens the G1 interval of the cell cycle. *J Biol Chem* **266:** 9194–9202

Muller EG (1996) A glutathione reductase mutant of yeast accumulates high levels of oxidized glutathione and requires thioredoxin for growth. *Mol Biol Cell* **7:** 1805–1813

Ojeda L, Keller G, Muhlenhoff U, Rutherford JC, Lill R, Winge DR (2006) Role of glutaredoxin-3 and glutaredoxin-4 in the iron regulation of the Aft1 transcriptional activator in Saccharomyces cerevisiae. *J Biol Chem* **281:** 17661–17669

Ortenberg R, Gon S, Porat A, Beckwith J (2004) Interactions of glutaredoxins, ribonucleotide reductase, and components of the DNA replication system of Escherichia coli. *Proc Natl Acad Sci USA* **101:** 7439–7444

Pocsi I, Prade RA, Penninckx MJ (2004) Glutathione, altruistic metabolite in fungi. *Adv Microb Physiol* **49:** 1–76

Pollard MG, Travers KJ, Weissman JS (1998) Ero1p: a novel and ubiquitous protein with an essential role in oxidative protein folding in the endoplasmic reticulum. *Mol Cell* **1:** 171–182

Puig S, Askeland E, Thiele DJ (2005) Coordinated remodeling of cellular metabolism during iron deficiency through targeted mRNA degradation. *Cell* **120:** 99–110

Pujol-Carrion N, Belli G, Herrero E, Nogues A, de la Torre-Ruiz MA (2006) Glutaredoxins Grx3 and Grx4 regulate nuclear localisation of Aft1 and the oxidative stress response in Saccharomyces cerevisiae. *J Cell Sci* **119**(Part 21)**:** 4554–4564

Rouhier N, Couturier J, Johnson MK, Jacquot JP (2009) Glutaredoxins: roles in iron homeostasis. *Trends Biochem Sci* **35:** 43–52

Rutherford JC, Jaron S, Winge DR (2003) Aft1p and Aft2p mediate iron-responsive gene expression in yeast through related promoter elements. *J Biol Chem* **278:** 27636–27643

Rutherford JC, Ojeda L, Balk J, Muhlenhoff U, Lill R, Winge DR (2005) Activation of the iron regulon by the yeast Aft1/Aft2 transcription factors depends on mitochondrial but not cytosolic iron-sulfur protein biogenesis. *J Biol Chem* **280:** 10135–10140

Sevier CS, Qu H, Heldman N, Gross E, Fass D, Kaiser CA (2007) Modulation of cellular disulfide-bond formation and the ER redox environment by feedback regulation of Ero1. *Cell* **129:** 333–344

Shakoury-Elizeh M, Tiedeman J, Rashford J, Ferea T, Demeter J, Garcia E, Rolfes R, Brown PO, Botstein D, Philpott CC (2004) Transcriptional remodeling in response to iron deprivation in Saccharomyces cerevisiae. *Mol Biol Cell* **15:** 1233–1243

Sharma KG, Sharma V, Bourbouloux A, Delrot S, Bachhawat AK (2000) Glutathione depletion leads to delayed growth stasis in Saccharomyces cerevisiae: evidence of a partially overlapping role for thioredoxin. *Curr Genet* **38:** 71–77

Shelton MD, Mieyal JJ (2008) Regulation by reversible S-glutathionylation: molecular targets implicated in inflammatory diseases. *Mol Cells* **25:** 332–346

Shi ZZ, Osei-Frimpong J, Kala G, Kala SV, Barrios RJ, Habib GM, Lukin DJ, Danney CM, Matzuk MM, Lieberman MW (2000) Glutathione synthesis is essential for mouse development but not for cell growth in culture. *Proc Natl Acad Sci USA* **97:** 5101–5106

Sipos K, Lange H, Fekete Z, Ullmann P, Lill R, Kispal G (2002) Maturation of cytosolic iron-sulfur proteins requires glutathione. *J Biol Chem* **277:** 26944–26949

Spector D, Labarre J, Toledano MB (2001) A genetic investigation of the essential role of glutathione: mutations in the proline biosynthesis pathway are the only suppressors of glutathione auxotrophy in yeast. *J Biol Chem* **276:** 7011–7016

Srikanth CV, Vats P, Bourbouloux A, Delrot S, Bachhawat AK (2005) Multiple cis-regulatory elements and the yeast sulphur regulatory network are required for the regulation of the yeast glutathione transporter, Hgt1p. *Curr Genet* **47:** 345–358

Toledano MB, Kumar C, Le Moan N, Spector D, Tacnet F (2007) The system biology of thiol redox system in Escherichia coli and yeast: differential functions in oxidative stress, iron metabolism and DNA synthesis. *FEBS Lett* **581:** 3598–3607

Travers KJ, Patil CK, Wodicka L, Lockhart DJ, Weissman JS, Walter P (2000) Functional and genomic analyses reveal an essential coordination between the unfolded protein response and ER-associated degradation. *Cell* **101:** 249–258

Trotter EW, Grant CM (2003) Non-reciprocal regulation of the redox state of the glutathione-glutaredoxin and thioredoxin systems. *EMBO Rep* **4:** 184–188

Wheeler GL, Trotter EW, Dawes IW, Grant CM (2003) Coupling of the transcriptional regulation of glutathione biosynthesis to the availability of glutathione and methionine via the Met4 and Yap1 transcription factors. *J Biol Chem* **278:** 49920–49928

Wimalasena TT, Enjalbert B, Guillemette T, Plumridge A, Budge S, Yin Z, Brown AJ, Archer DB (2008) Impact of the unfolded protein response upon genome-wide expression patterns, and the role of Hac1 in the polarized growth, of Candida albicans. *Fungal Genet Biol* **45:** 1235–1247

Wu AL, Moye-Rowley WS (1994) GSH1, which encodes gamma-glutamylcysteine synthetase, is a target gene for yAP-1 transcriptional regulation. *Mol Cell Biol* **14:** 5832–5839

Yamaguchi-Iwai Y, Ueta R, Fukunaka A, Sasaki R (2002) Subcellular localization of Aft1 transcription factor responds to iron status in Saccharomyces cerevisiae. *J Biol Chem* **277:** 18914–18918

Yun CW, Ferea T, Rashford J, Ardon O, Brown PO, Botstein D, Kaplan J, Philpott CC (2000) Desferrioxamine-mediated iron uptake in Saccharomyces cerevisiae. Evidence for two pathways of iron uptake. *J Biol Chem* **275:** 10709–10715

